

Variation of the Density of States in Amorphous GdSi at the Metal-Insulator Transition

L. Bokacheva^a, W. Teizer^b, F. Hellman^a, and R. C. Dynes^a

^a*Department of Physics, University of California, San Diego, La Jolla, CA 92093-0319*

^b*Department of Physics, Texas A&M University, College Station, TX 77843-4242*

(Dated: October 10, 2003)

We performed detailed conductivity and tunneling measurements on the amorphous, magnetically doped material α -Gd_xSi_{1-x} (GdSi), which can be driven through the metal-insulator transition by the application of an external magnetic field. Conductivity increases linearly with field near the transition and slightly slower on the metallic side. The tunneling conductance, proportional to the density of states $N(E)$, undergoes a gradual change with increasing field, from insulating, showing a soft gap at low bias, with a slightly weaker than parabolic energy dependence, i.e. $N(E) \sim E^c$, $c \lesssim 2$, towards metallic behavior, with E^d , $0.5 < d < 1$ energy dependence. The density of states at the Fermi level appears to be zero at low fields, as in an insulator, while the sample shows already small, but metal-like conductivity. We suggest a possible explanation to the observed effect.

PACS numbers: PACS: 75.50.Pp, 71.23.Cq, 71.30.+h

I. INTRODUCTION

The metal-insulator transition (MIT) in disordered systems¹ is a complex problem, complete and accurate treatment of which requires that the effects of localization and the electronic correlations be taken into account simultaneously and on equal footing. The main difficulty in constructing such a model lies in the fact that near the MIT strong Coulomb interactions cannot be treated perturbatively and thus render single-particle models unrealistic. Carriers that are localized by the disordered potential cannot screen the Coulomb interactions as well as the mobile ones, therefore in disordered systems the correlations play an important role and must be included in the picture of the MIT.

Far from the transition, theoretical models have successfully described the effects due to the interactions in the conductivity σ and density of states (DOS) $N(E)$. The transport conductivity of a metallic material with strong Coulomb correlations as a function of temperature follows a power law: $\sigma(T) = \sigma_0 + \sigma_1 T^y$, with $y = 0.5$.² On the insulating side, the interactions modify the exponent of the temperature dependence of the variable range hopping (VRH) conductivity from 1/4 in the noninteracting case³ to 1/2: $\sigma(T) \sim \exp(-(T_0/T)^{1/2})$.⁴ In the density of states, on either side of the MIT, interactions generally cause the depletion of states near the Fermi energy. In the metallic regime the correlations are manifested as a square-root dip in the DOS: $N(E) = N(0)(1 + (E/\Delta)^{1/2})$, where $\Delta \sim \hbar D/l^2$ is the correlation energy, D is the diffusion coefficient, l is the mean free path, and \hbar is Planck's constant.^{5,6} In an insulator with thermally activated variable range hopping conductivity, the interactions lead to the opening of a soft gap with a quadratic (in 3D case) energy dependence, $N(E) = (3/\pi)(\kappa/e^2)^3 E^2$, where κ is the dielectric constant and e is the electronic charge. The width of the Coulomb gap⁷ Δ_c is determined by κ and the noninteracting density of states N_0 : $\Delta_c = e^3(N_0/\kappa^3)^{1/2}$.

The presence of the features due to the Coulomb interactions in the conductivity and the DOS of disordered systems near the MIT has been well established experimentally. The usual way to investigate the transition is to study a set of samples with different dopant concentrations near the critical one.⁸ In these samples one can measure the transport conductivity and in some cases, the tunneling conductance, which is believed to be approximately proportional to the DOS. Features described above, such as VRH with 1/2 exponent, the Coulomb gap in the DOS on the insulating side, the square root of T conductivity dependence and the square root cusp in the DOS have been observed in various experiments performed on crystalline⁹ and amorphous samples.¹⁰

Amorphous systems have an advantage over the crystalline materials for the MIT studies, since they undergo the transition at doping concentrations that are orders of magnitude higher than the crystalline materials (roughly $x \sim 10^{-1}$ versus $x \sim 10^{-5}$). As a consequence, the Fermi temperature T_F of amorphous systems is much higher than in the crystalline ones, and T/T_F is much lower. While it becomes inappropriate to think in terms of single particles, it is convenient to use the terminology to identify the conditions where these correlation effects dominate. For amorphous systems the region where the Ioffe-Regel localization criterion¹¹ $k_F l \sim 1$ is valid (here k_F is the Fermi wave vector) is significantly expanded, and the maximum critical conductivity $\sigma = ne^2/(\hbar k_F^2)$, where n is the concentration, can reach $500 (\Omega \text{ cm})^{-1}$ at $n \sim 10^{22} \text{ cm}^{-3}$, as opposed to $20 (\Omega \text{ cm})^{-1}$ in the crystalline doped semiconductors.⁸ Therefore, in amorphous materials one can probe the transition much deeper in the critical regime at accessible temperatures.

In some materials it is possible to observe the MIT in a single sample and tune it by varying an external parameter, such as magnetic field,¹² stress,¹³ or illumination.¹⁴ This approach is preferable to studying multiple samples, because it eliminates the undesirable scatter in the sample parameters, inevitable when using a discrete set of

samples. For this reason, magnetically doped amorphous materials, such as α -Gd $_x$ Si $_{1-x}$ (GdSi) and Tb $_x$ Si $_{1-x}$,^{15,16} are particularly suited for the studies of the MIT. In these materials besides the structural disorder, there is an additional degree of disorder associated with random orientation of the ionic magnetic moments, which can be controlled by the magnetic field. When the magnetic moments of the impurity ions are aligned by the external field, the disorder in the system is reduced, and the mobility edge E_c is lowered.¹⁷ This promotes delocalization of carriers and increases the conductivity of the material. Therefore a single sample with the concentration slightly below critical and thus insulating can be continuously driven through the MIT into the metallic state by an external magnetic field. It is also possible to probe the density of states (DOS) simultaneously with the transport properties of these materials by studying the tunneling of quasiparticles through a thin oxide barrier between the material in question and a metallic electrode. These experiments enable one to track the changes that occur in the DOS at the transition and to separate them from the mobility effects, which both contribute to the conductivity.

Insulating and metallic behavior can be defined as follows. The sample is an insulator, if its conductivity $\sigma(T)$ extrapolated to zero temperature vanishes: $\sigma(T = 0) = 0$. If $\sigma(T = 0)$ is finite, the sample is on the metallic side of the transition. In GdSi the MIT occurs at $x \approx 0.14$ of Gd in zero magnetic field. Near this critical doping value, $\sigma(T = 0)$ is very sensitive to the slight variations of x . A sample doped slightly below the critical level at low temperature shows a large positive magnetoconductivity and can be continuously driven through the transition by the magnetic field.¹⁸ Near the MIT the amorphous GdSi has been extensively studied: its structure,¹⁹ transport conductivity,^{15,18,20} tunneling conductance,^{17,21} specific heat,²² magnetization,²³ infrared absorption,²⁴ spin polarization,²⁵ and the Hall effect,²⁶ have been investigated in detail. It has been shown that the magnetic field plays a role similar to increasing the Gd concentration x and increases the conductivity while raising both the free carrier concentration and the density of states, which appear to grow towards the metallic side in a coordinated way.¹⁷ In further work the density of free carriers has been found to vary linearly with magnetic field.²⁶

The results of tunneling measurements¹⁷ indicate that deep in the metallic regime, yet at σ_0 still below the Ioffe-Regel condition, the DOS of GdSi has $E^{1/2}$ dependence with a non-vanishing $N(0)$. Tunneling conductance curves $dI/dV(V)$ at different constant magnetic fields are approximately parallel to each other with only $N(0)$ increasing with field. On the insulating side these experiments are limited by the increasing resistance of the GdSi film. When the resistance of the insulating GdSi film over the area of the tunnel junction becomes comparable with the resistance of the junction itself, the voltage drop occurs both over the junction and the film, so that

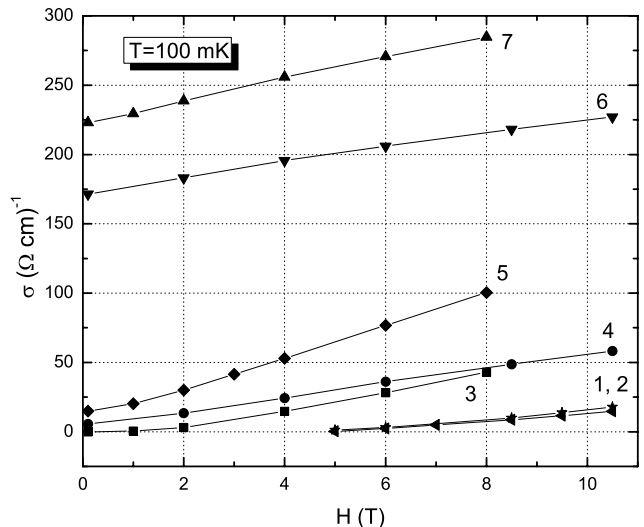


FIG. 1: Low temperature conductivity $\sigma(H)$ of seven different samples versus the applied magnetic field. At $H = 0.1$ T samples #1 and #2 are insulating, sample #3 is at the transition, samples #4 and #5 are slightly metallic, samples #6 and #7 are in the metallic regime.

the bias voltage cannot be considered a true energy coordinate. In samples which become conducting in magnetic field, the DOS shows a soft gap near zero bias with somewhat weaker than E^2 dependence and $N(0)$ vanishing at low fields. The tunneling data also suggest that in the transition region the DOS evolves continuously from insulating, showing a soft gap at zero bias, to metallic, with a square root cusp, upon increasing magnetic field. Near the MIT the DOS at the Fermi level $N(0)$ has been shown to depend on magnetic field as $(H - H_c)^2$.¹⁷ The models for the DOS described above that are valid far from the transition, cannot be applied in the critical region and cannot be properly merged at the critical concentration. It is not known how the DOS evolves from the insulating form to the metallic one. It is therefore highly desirable to be able to tune a single sample through the MIT and measure its transport and tunneling properties as close to the transition as possible.

II. EXPERIMENTAL RESULTS

In this paper we focus on the region in the immediate vicinity of the MIT and investigate the simultaneous variation of the transport conductivity and the DOS in a detailed and systematic way. The results presented here were obtained using GdSi samples prepared as described previously.¹⁷ Amorphous films of GdSi, 100 nm thick, have been grown by e-beam co-evaporation on Si/SiN substrates. On top of the GdSi film tunnel junctions were formed with a thermally grown oxide barrier and Pb counter electrodes. The tunnel junctions were also used as voltage terminals in the four point transport measure-

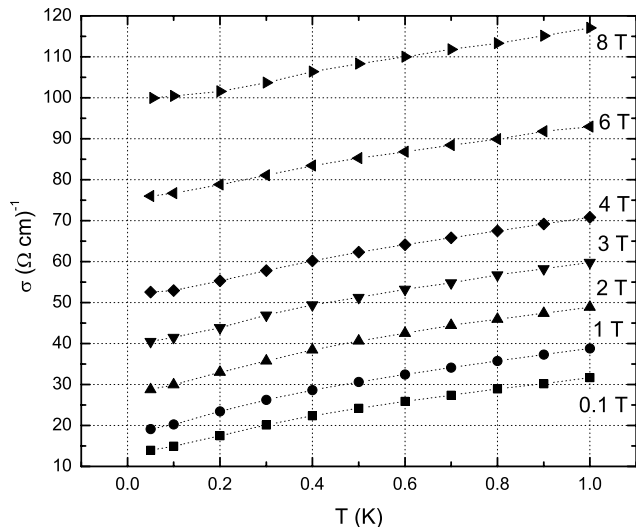


FIG. 2: Conductivity of a slightly metallic GdSi sample (sample #5) versus temperature.

ments. We selected only those samples, for which the junction resistance was at least an order of magnitude higher than the film resistance over the area of the junction.

A. Transport conductivity measurements

At low temperatures (below approximately 50 K) GdSi shows a large positive magnetoconductance.²⁰ In order to determine the sample's proximity to the MIT and to avoid the ambiguity associated with the extrapolation of $\sigma(T)$ to $T = 0$, we use the actual conductivity values at the lowest temperatures available in our experiments (≤ 100 mK). The relative increase of the conductivity with field is the largest in the insulating samples, where the conductivity grows as a faster than linear function of the applied field. In samples which are right at the transition or barely on the metallic side, the conductivity at a constant low temperature increases approximately linearly with magnetic field. Far on the metallic side this dependence is slightly weaker than linear. Fig. 1 shows the low temperature ($T = 100$ mK) conductivity versus the applied magnetic field for several different samples, with the conductivity spanning a broad range from zero to over $200 (\Omega \text{ cm})^{-1}$, all below the Ioffe-Regel limit.

The conductivity of the most insulating samples #1 and #2 becomes measurable above 4 – 5 T and grows rapidly with field from nearly zero ($0.4 (\Omega \text{ cm})^{-1}$) to $14 - 17 (\Omega \text{ cm})^{-1}$ at $H = 10.5$ T, i.e., between the lowest and the highest field the conductivity in these samples increases by 40 or 50 times. Sample #3 is very close to the transition, and samples #4 and #5 are barely on the metallic side of the MIT. The conductivity of samples #3, #4 and #5 is approximately linear with field. In sample #3 the conductivity grows between 0.1 T and 8 T by

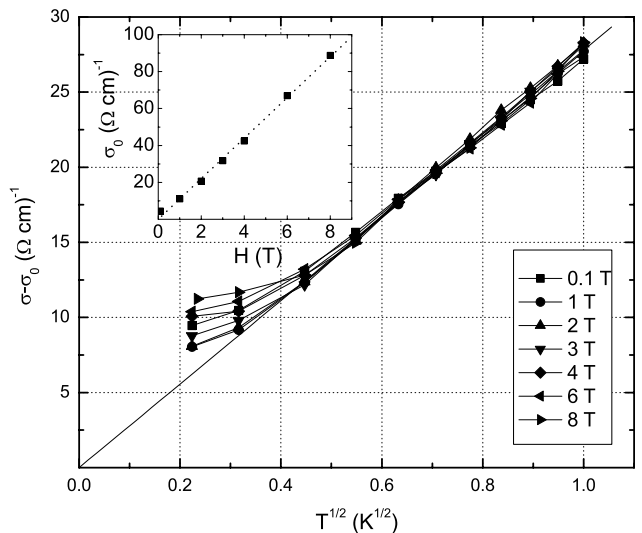


FIG. 3: Conductivity $\sigma - \sigma_0$ from the data on Fig. 2 versus $T^{1/2}$ with σ_0 determined from linear fits to $\sigma(T^{1/2})$ subtracted. Solid line is a linear fit to the data. Inset: σ_0 vs magnetic field H . Dotted line is a linear fit.

a factor of 40. The increase in the conductivity becomes much smaller for slightly metallic samples #4 and #5, in which it increases by a factor of 10 and 7 respectively. Conductivity of the most metallic samples #6 and #7 is a slightly sublinear function of the field ($\sim H^{0.85}$) and in the shown range of field increases only by about 25% of its value at $H = 0.1$ T.

Fig. 2 shows the conductivity versus temperature curves for the barely metallic sample #5 ($\sigma(50 \text{ mK}) = 14 (\Omega \text{ cm})^{-1}$) obtained from the dc IV transport measurements at constant fields from 0.1 T to 8 T. As shown before,¹⁷ the conductivity curves can be fit with the power law $\sigma(T) = \sigma_0 + \sigma_1 T^y$ with the exponent $y \approx 0.6 - 0.7$, slightly higher than the predicted $y = 0.5$ for a metal with correlations. The curves at different fields are approximately parallel to each other, only shifted towards higher values, which implies that σ_0 grows roughly linearly with field, as illustrated on Fig. 1, and σ_1 is weakly dependent on H . This can be easily seen in Fig. 3, which shows the same data as in Fig. 2, plotted as a function of $T^{1/2}$. The lowest temperature offset σ_0 , in this case determined from the linear fits to $\sigma(T^{1/2})$, has been subtracted from each curve. The linear variation of σ_0 with field is shown in the inset of Fig. 3. The $\sigma(T^{1/2})$ data at different fields overlap well and except at the lowest temperatures, fall onto a straight line. This dependence has been observed in non-magnetic materials, which supports the idea that the main effect of the applied magnetic field is to decrease the disorder and lower the mobility edge, thus increasing the conductivity and driving the sample further into the metallic regime.

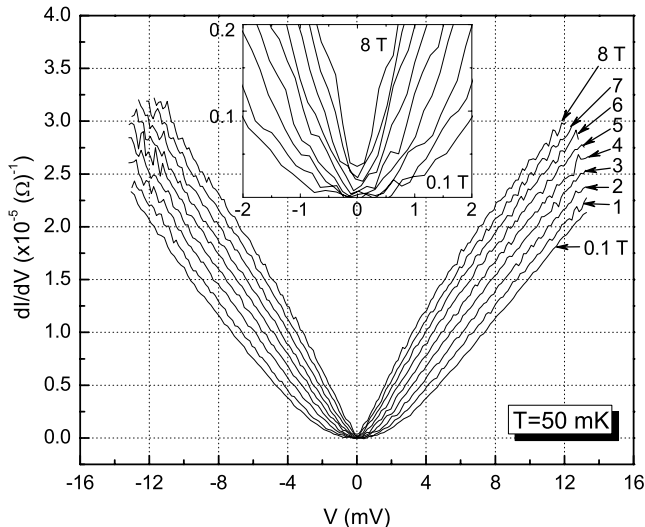


FIG. 4: Tunneling conductance $dI/dV(V)$ curves at $T = 50$ mK and different magnetic fields. Inset: Same data in the low bias region. The axes are in the same units as the main figure.

B. Tunneling conductance measurements

To elucidate the crossover in the DOS from the insulating to the metallic behavior we performed detailed tunneling studies. The data presented below are the results of the dc IV measurements. The dc technique is more appropriate in this case because at low temperatures near the MIT the resistance and the dielectric constant of GdSi films are strongly frequency dependent. The IV curves measured at constant magnetic fields and a constant low temperature were numerically differentiated in order to obtain the differential tunneling conductance $dI/dV(V)$. Fig. 4 shows a set of such curves for sample #5 at 50 mK and magnetic fields from 0.1 T to 8 T.

At the lowest field $H = 0.1$ T (required to quench the superconductivity of the Pb counter electrodes) the tunneling conductance curve is superlinear in the whole range of the bias voltage between ± 12 mV, but cannot be fit with a simple function. Near zero bias at $|V| < 2.5$ mV the curve can be fit with a power law $a + b|V|^c$, with $c \sim 1.72$. Outside this region the exponent c is only slightly greater than unity: $c \sim 1.1$. At $V = 0$ the curve touches the horizontal axis, i.e. zero bias conductance is unmeasurably small: $dI/dV(V = 0) = 0$. Upon increasing the field, the curves undergo a gradual and continuous change. The gap region with $c \gtrsim 1.5$ contracts and by 8 T it exists only in a small interval at $|V| < 0.6$ mV. The part of the curve at higher bias expands and at the same time the exponent c in this region decreases from nearly unity at 0.1 T to 0.74 at 8 T, apparently approaching the $V^{1/2}$ behavior seen well into the metallic regime. Starting at about $H = 2$ T, the dI/dV curves have an inflection point, separating the two parts of the curve with

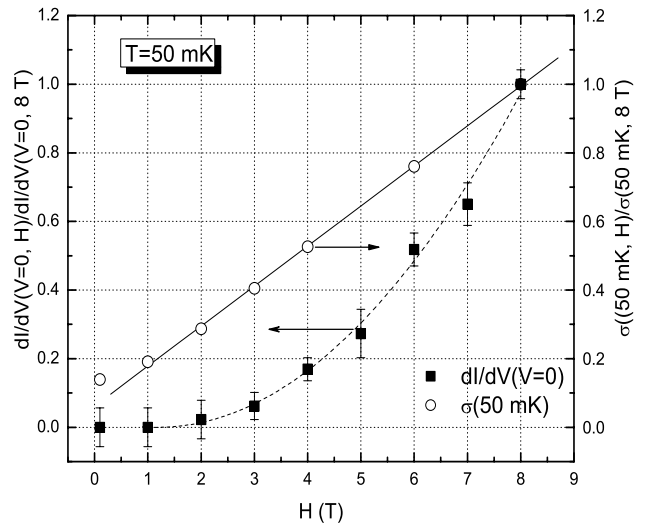


FIG. 5: Zero bias conductance $dI/dV(V = 0)$ (full squares) from the data on Fig. 4 and conductivity at $T = 50$ mK (empty circles), both normalized to their respective values at $H = 8$ T, versus magnetic field. Dashed line is the fit of $dI/dV(V = 0)$ with $0.02 \times (H - 1.2)^2$. Solid line is a linear fit to $\sigma_0(H)$.

$c > 1$ (positive curvature), implying a “soft gap” and $c < 1$ (negative curvature). At the highest field $H = 8$ T, the dI/dV curve is sublinear almost in the entire range of the bias voltage except a small region of $|V| < 0.6$ mV near zero, and is characteristic of the metallic regime.

This continuous crossover can be seen in more detail in the inset of Fig. 4, which shows a zoom-in of the data in the low bias region below 2 mV. Zero bias conductance appears to be zero at 0.1 T and $H = 1$ T, but increases at higher fields. In Fig. 5 zero bias conductance, normalized to its value at 8 T, is plotted versus H and can be well fit with $(H - H_c)^2$ with $H_c \approx 1.2$ T. Note that while $dI/dV(V = 0) \sim N(0) \approx 0$ at the two lowest fields, 0.1 T and 1 T, the sample has already an appreciable transport conductivity, 14 and 19 $(\Omega \text{ cm})^{-1}$ respectively (see also Fig. 2). At these fields the sample exhibits metallic transport properties, but appears to have an unmeasurably small number of extended states at the Fermi level from the tunneling experiments.

The gradual change in the shape of the $dI/dV(V)$ curves from an insulating V^2 to a metallic $V^{1/2}$ dependence and the position of the inflection point can be easily seen on a plot of the second derivative of the IV curves, $d^2I/dV^2(V)$ shown on Fig. 6. The d^2I/dV^2 curves reflect the curvature of the IV and the slope of the dI/dV curves. Clearly, the curvature is the largest and positive in the region near zero bias. With increasing field this region shrinks, and the point of inflection moves to lower voltage values. The maximum in d^2I/dV^2 corresponds to the change of curvature in the dI/dV from positive to negative. In order to determine the position of the inflection point in dI/dV , we take a maximum of the d^2I/dV^2

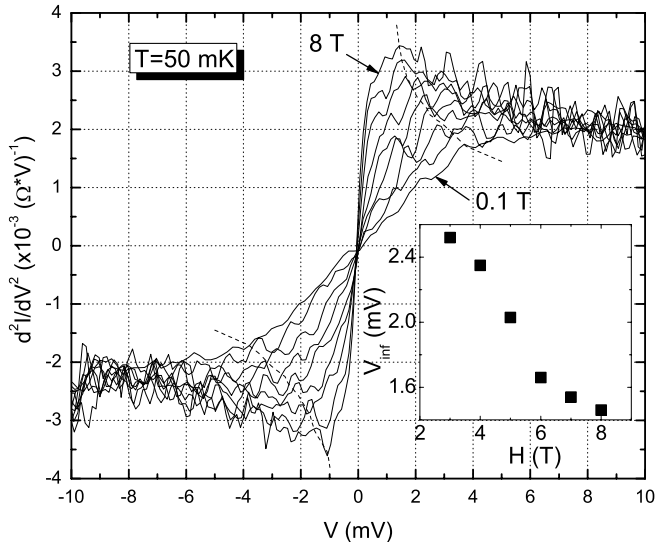


FIG. 6: Second derivative of the IV , $d^2I/dV^2(V)$ for the data on Fig. 4. Dashed line is a guide for the eye indicating the position of a maximum shifting to lower bias with increasing field. Inset: The bias voltage V_{inf} at which the inflection point in the dI/dV curves is located, plotted versus magnetic field.

on Fig. 6. The curves at the lowest fields, 0.1 T and 1 T, do not have a maximum, although their slope significantly decreases at 3.75 mV and 3.6 mV respectively and falls almost to zero above 6 mV. Upon increasing the field, a maximum appears in the d^2I/dV^2 curve, which corresponds to an inflection point in dI/dV , and moves towards $V = 0$. The bias voltage, at which the inflection occurs, decreases with increasing field, as shown in the inset of Fig. 6.

The significance of these data, we believe, is the indication that the crossover from metallic $V^{1/2}$ behavior to insulating V^2 behavior is continuous and we cannot identify from the tunneling data a “critical point” that marks the transition.

We emphasize that this study probes the sample very close to the MIT with high resolution. This is achieved for two reasons. Firstly, the transition is continuously tuned with applied field, and secondly, the region of study is well below the Ioffe-Regel condition. We have observed similar behavior in the tunneling characteristics of all samples studied to date in the vicinity of the MIT. In fact, the $dI/dV(V)$ data at different fields for different samples can be scaled to form one “master set” of curves, progressively changing their shape from insulating to metallic, correlated with the sample conductivity.

The results of the tunneling experiments can be summarized as follows. The DOS evolves gradually and continuously with increasing magnetic field from an insulating to a metallic shape. The Coulomb correlation gap, associated with the insulating behavior, shrinks as the field increases. At these fields, transport experiments on the sample already show metallic transport conductiv-

ity. Zero bias tunneling conductance grows as a strong (quadratic) function of the applied field. For samples very close to the transition, one can observe a situation, where the tunneling conductance is vanishingly small, and the transport conductivity is already appreciable. This is a result we did not expect, as we anticipated that $N(E)$ and σ_0 would vanish together at the transition. We conclude that the effects in the density of states $N(E)$ that are associated with the insulating regime persist well into the metallic regime.

III. DISCUSSION

Observation of a measurable metallic conductivity simultaneously with an apparent absence of the extended states at the Fermi level appears paradoxical at first sight. Nevertheless, a situation where this is possible can be easily pictured. Consider a strongly disordered system approaching the MIT from an insulating side. When at the transition a small fraction of all carriers becomes delocalized, the current may flow via a very small number of conduction paths among the disordered sites. Conductivity due to these paths is much higher than that due to the rest of the carriers, which are still localized and participate in transport by the thermally activated variable-range hopping. At low temperature the contribution of the localized carriers to the conductivity is exponentially small compared to the contribution of the extended states, despite the fact that the former constitute an overwhelming majority among all carriers. The overall conductivity therefore will be determined by the few, high mobility extended carriers. On the other hand, the DOS that is observed in an experiment, such as ours, reflects an average number among all microscopic states in the sample at a given energy, thus its magnitude will be determined by the dominating species. Near the transition a small number of carriers possess a metallic DOS with $N(E) \sim E^{1/2}$ and $N(0) \neq 0$, however a vast majority of states still show an insulating type of DOS with a parabolic energy dependence and a vanishing $N(0)$. When summed over all microscopic states with appropriate weights proportional to the numbers of each species, the contribution to the DOS of the localized states overwhelmingly prevails over that of the metallic ones, and as a result, at the transition the total DOS appears to be insulating. In this case the DOS at $E = 0$ at the MIT is likely to vanish. As the sample is driven towards the metallic regime and the number of the extended carriers grows, the DOS acquires an intermediate shape, i.e., it shows features due to both insulating and metallic species simultaneously. Gradually the signatures of the metallic behavior begin to take over larger and larger range of energy, until eventually they dominate the whole DOS. At the same time, while the sample is tuned into the metallic regime, its conductivity rapidly increases and exhibits metallic behavior. Therefore, it is plausible that in the same conditions, the transport experiments will

place this sample on the metallic side of the transition, while in the tunneling measurements it will appear as an insulator.

It could be argued that this description is a percolation transition on an atomic scale and that a percolation threshold in a two component system in 3 dimensions should occur at a fractional concentration of $x_c \sim 0.43$ (for site percolation in a diamond structure).²⁷ However this transition must take into account in addition to the natural inhomogeneity at the atomic scale, the strong correlations that are ignored in a classical model. Indeed, while we resort to a single particle picture of mobility and density of states for descriptive reasons, we must remind ourselves that this transition is believed to be driven by the correlations which are not single particle effects. We

believe that these current experiments show that thinking in terms of independent particles in the vicinity of the metal-insulator transition, despite the convenience of using such pictures, is an oversimplification. Further theoretical work may be able to put these experimental results on a solid footing within the correlation-based models.

Acknowledgments

We thank S. Kivelson, O. Naaman, and A. Frydman for valuable discussions. This work was supported by the NSF Grant No. DMR-0097242.

-
- ¹ P. A. Lee and T. V. Ramakrishnan, *Rev. Mod. Phys.* **57**, 287 (1985); B. Kramer and A. McKinnon, *Rep. Prog. Phys.* **56**, 1469 (1993); N. F. Mott, *Conduction in Non-Crystalline Materials* (Clarendon Press, Oxford, 1993).
- ² B. L. Altshuler and A. G. Aronov, *JETP Lett.* **30** (1979), 514; B. L. Altshuler, D. Khmel'nitzkii, A. I. Larkin and P. A. Lee, *Phys. Rev. B* **22** (1980), 5142.
- ³ N. F. Mott, *J. Non-Cryst. Solids* **1**, 1 (1968).
- ⁴ A. L. Efros and B. L. Shklovskii, *J. Phys. C* **8**, L49 (1975).
- ⁵ B. L. Altshuler and A. G. Aronov, *Solid State Commun.* **30**, 115 (1979); B. L. Altshuler and A. G. Aronov, *Sov. Phys. JETP* **50**, 968 (1979).
- ⁶ W. L. McMillan, *Phys. Rev. B* **24**, 2739 (1981).
- ⁷ B. L. Shklovskii and A. L. Efros, *Fiz. Tekh. Poluprovodn.* **14**, 825 (1980) [*Sov. Phys. Semicond.* **14**, 487 (1980)].
- ⁸ T. F. Rosenbaum, K. Andres, G. A. Thomas, and R. N. Bhatt, *Phys. Rev. Lett.* **45**, 1723 (1980); B. W. Dodson et al., *Phys. Rev. Lett.* **46**, 46 (1981); W. N. Shafarman, D. W. Koon, and T. G. Castner, *Phys. Rev. B* **40**, 1216 (1989).
- ⁹ J. G. Massey and Mark Lee, *Phys. Rev. Lett.* **75**, 4266 (1995); *ibid.* **77**, 3399 (1996); *ibid.* **79**, 3986 (1997); Mark Lee and J. G. Massey, V. L. Nguyen and B. I. Shklovskii, *Phys. Rev. B* **60**, 1582 (1999); J. G. Massey and Mark Lee, *Phys. Rev. B* **62**, R13270 (2000).
- ¹⁰ G. Hertel, D. J. Bishop, E. G. Spencer, J. M. Rowell, and R. C. Dynes, *Phys. Rev. Lett.* **50**, 743 (1983); D. J. Bishop, E. G. Spencer, and R. C. Dynes, *Solid State Electron.* **28**, 73 (1985).
- ¹¹ A. F. Ioffe and A. R. Regel, *Prog. Semicond.* **4**, 237 (1960).
- ¹² S. von Molnar and S. Methfessel, *J. Appl. Phys.* **38**, 959 (1967); S. von Molnar, A. Briggs, J. Flouquet, and G. Remenyi, *Phys. Rev. Lett.* **51**, 706 (1983); S. Washburn, R. A. Webb, S. von Molnar, F. Holtzberg, J. Flouquet, and G. Remenyi, *Phys. Rev. B* **30**, 6224 (1984); J. Jaroszynski and T. Dietl, *Physica (Amsterdam)* **177B**, 469 (1992).
- ¹³ M. A. Paalanen, T. F. Rosenbaum, G. A. Thomas and R. N. Bhatt, *Phys. Rev. Lett.* **48**, 1284 (1982); S. Waffenschmidt, C. Pfeleiderer, and H. v. Löhneysen, *ibid.* **83**, 3005 (1999).
- ¹⁴ I. Terry, T. Penney, S. von Molnar, J.M. Rigotty, and P. Becla, *Solid State Commun.* **84**, 235 (1992); C. Leighton, I. Terry and P. Becla, *Europhys. Lett.* **42**, 67 (1998); *Phys. Rev. B* **58**, 9773 (1998).
- ¹⁵ F. Hellman, M. Q. Tran, A. E. Gebala, E. M. Wilcox, and R. C. Dynes, *Phys. Rev. Lett.* **77**, 4652 (1996).
- ¹⁶ M. Liu and F. Hellman, *Phys. Rev. B* **67**, 054401 (2003).
- ¹⁷ W. Teizer, F. Hellman, and R. C. Dynes, *Phys. Rev. Lett.* **85**, 848 (2000).
- ¹⁸ W. Teizer, F. Hellman, and R. C. Dynes, *Solid State Commun.* **114**, 81 (2000).
- ¹⁹ F. Hellman, W. Geerts, and B. Donehew, *Phys. Rev. B* **67**, 012406 (2003).
- ²⁰ P. Xiong, B. L. Zink, S. I. Applebaum, F. Hellman, and R. C. Dynes, *Phys. Rev. B* **59**, R3929 (1999).
- ²¹ W. Teizer, F. Hellman and R. C. Dynes, in *Proceedings of the 25th International Conference on the Physics of Semiconductors, Osaka, 2000*, edited by N. Miura and T. Ando (Springer, 2000).
- ²² B. L. Zink, E. Janod, K. Allen, and F. Hellman, *Phys. Rev. Lett.* **83**, 2266 (1999).
- ²³ F. Hellman, D. R. Queen, R. M. Potok, and B. L. Zink, *Phys. Rev. Lett.* **84**, 5411 (2000).
- ²⁴ D. N. Basov, A. M. Bratkovsky, P. F. Henning, B. Zink, F. Hellman, C. C. Homes, and M. Strongin, *Europhys. Lett.* **57**, 240 (2002).
- ²⁵ W. Teizer, F. Hellman and R. C. Dynes, *Int. J. Mod. Phys. B* **17**, 3723 (2003) and unpublished.
- ²⁶ W. Teizer, F. Hellman, and R. C. Dynes, *Phys. Rev. B* **67**, R121102 (2003).
- ²⁷ R. Zallen, *The Physics of Amorphous Solids*, p. 170 (Wiley, New York, 1983).